J. Math. Computer Sci., 37 (2025), 45–58

Online: ISSN 2008-949X

Journal of Mathematics and Computer Science

Journal Homepage: www.isr-publications.com/jmcs

Caputo fractal-fractional mathematical study of SIS epidemic dynamical problem with competitive environment and neural network

M. A. El-Shorbagy[a,b], Mati ur Rahman[c,d,*], Muhammad Arfan[e]

[a]Department of Mathematics, College of Science and Humanities in Al-Kharj, Prince Sattam bin Abdulaziz University, Al-Kharj 11942, Saudi Arabia.

[b]Department of Basic Engineering Science, Faculty of Engineering, Menoufia University, Shebin El-Kom 32511, Egypt.

[c]School of Mathematical Sciences, Jiangsu University, Zhenjiang 212013, Jiangsu, P.R. China.

[d]Department of computer science and mathematics, Lebanese American university, Beirut, Lebanon.

[e]Department of Mathematics, Government Degree College Gulabad Dir(L), Khyber Pakhtunkhwa, Pakistan.

Abstract

The infection of any disease is one of the most highly affected factors for the dynamics of all species population and this may be for the case of human populations throughout the world. The infection of any disease acts like a predator or competitor for the healthy population or species of the environment. In this article, the dynamics of one type of species' density are investigated by the spreading of infection in the environment along with competition with other species and among themselves. The generalized operator in the sense of Caputo having fractal dimension and non-integer order is operated to consider the problem for testing the complex geometry of the said dynamics. The total density of the species is divided into two agents of healthy class and the infectious class. For the biological validation, the qualitative analysis is carried out in the sense of fixed point theory. The stability analysis for the solution is also treated by using the Ulam-Hyers concept of stability in the sense of the said operator. The numerical scheme has been developed for each quantity along with a graphical representation of different fractional order and fractal dimensions. Using an artificial neural Network (ANN) technique, we have divided the data set into three different categories in this study: training, testing, and validation. This study includes a detailed analysis that we conducted based on this division.

Keywords: Mathematical model, numerical solution, artificial neural network, competitive species, qualitative analysis.

2020 MSC: 68T07, 37N25.

1. Introduction

The transmission of infection of various diseases up to date implies a basic issue due to two reasons, one is of species existence and the other one is of the balance of different biological or ecosystems. Many scientific Technique are introduced to find best approaches for the suppressions and controlling of the diseases [12]. One of the significant and more beneficial way is of mathematical modeling in deterministic

*Corresponding author
Email address: matimaths@ujs.edu.cn (Mati ur Rahman)

doi: 10.22436/jmcs.037.01.04

Received: 2024-02-23 *Revised:* 2024-04-13 *Accepted:* 2024-07-29

form for treating the epidemiological dynamics which is very effective for understanding the connections of disease transmission and perform the suitable control methods [11, 16, 34]. Among them are the basic predator-prey or competitive models extended to Epidemiology problems given in [18] as a development of the continuous-time deterministic models using mostly the Natural first-order differentiation. Such models are significantly constructed in various ways like the continuous-time single population of species having epidemiological mathematical form with natural derivative of order one [13, 23, 25, 30], the counting-five times uni-population species epidemiology dynamics [15, 22, 26], the probabilistic uni-specie model of epidemiology [27, 38], and the time dependent models of Eco-epidemiology [9, 19, 24].

Since 1990, the area of modern calculus have achieved vast interest from the sides of mathematicians. Famous scholars of mathematics have given their work in this field by incorporating various modern operators of derivatives and antiderivatives in different research papers. The afore said calculus of integration and integration provided comparative with real world outcomes as measured by the integer order derivative. It investigates the dynamical behavior of real globe problems for the non-integer order. The fractional operations have extra choices for selection and it generalized the natural order differentiation and integrals formulae. The modern world scholars have written papers, monographs, articles, and different chapters which include the aforesaid field. The diagrammatical and physical interpretation of the arbitrary derivative order was given by Podlubny [32]. Study of different dynamics related to real life systems under the modern operators can be searched in [21, 37]. The usages of the aforesaid field in engineering with more detail is given in [17]. Also more kinds of research articles have published having their composition are of qualitative analysis and numerical study under the globalized operators. Among the founders of fractional calculus is Riemann-Liouville who gives the first formulation of fractional derivatives in 1832. After him different researchers made their contribution in this aspects. In 1967, the aforesaid formula was further simplified by Caputo, vastly applied in searching global phenomena.

Some researchers developed the model of epidemiology like the SIR model as in [18]. For one-type species situation, the said model is only treated for the infection that is present in the human populations densities. As, infections also affect the presence of the wild species population densities which interrupt the stability of the eco-system, for instance, the infections in epidemic species like Orangutans [31], Tarsius [4], Sumatran Tiger [29], and Komodo dragon [35]. Furthermore, the natural environment dynamics of animals that threaten the presence of their densities are the intra specific competitive result among them to preserve sources of their food web or food chain [2, 10, 28]. They considered the aforesaid points for the models of epidemiology as their contribution in this aspect having the mathematical model [14] as follows:

$$
\begin{aligned}
\dot{S}(t) &= (r-\mu)S(t) - \Omega_1 S^2(t) - (\Omega_2+\beta)S(t)I(t) + \eta I(t),\\
\dot{I}(t) &= (\beta-\Omega_4)S(t)I(t) - \Omega_3 I(t)^2 - (\eta+\mu)I(t),
\end{aligned}
\tag{1.1}
$$

where $S(t)$ is susceptible class, $I(t)$ is infected class, r is the recruitment rate, μ is the natural occurring rate of death, Ω_1 is the death rate of $S(t)$ due to its same competitors, Ω_2 is the rate of death of same class due to other competitors, Ω_3 is death rate infected class due its same competitors, Ω_4 the death rate of same class due to other competitors, η is rate of recovery, and β is the rate infection.

In 2015, a novel formula for Caputo-Fabrizio (CF) differentiation was given by Fabrizio and Caputo by changing the power law kernel of singularity in the pre-defined formula by exponential non singular kernel. For applications of the said operator, we reference the readers to study [8, 33, 36]. After one year of that, in 2016 Baleanu and abdon Atangana under Caputo, converted the CF to ABC kind of operator. This novel operator has been applied very well in different aspects globalized problems as given in [1, 20]. It is often challenging to provide an exact classical derivative formulation for biological mathematical problems due to the presence of complex and extraneous data. In such cases, generalized operators, which account for power-law behaviors and fading memory effects, can be beneficial. Moreover, models with complex geometries may not be well-suited for a direct application of power-law and fading memory principles. For obtaining this problem a novel defined formula of fractional-fractal may be beneficial to treat such kind of problems related to mathematics [7]. Few years before, Atangana gave a novel fractiona-fractal formula and provided the relation between fractional and fractal modern calculus [6]. Many scholars use this novel formula to various models in global life as can be seen in [3, 6]. By application of the fractal dimensional and fractional order derivative for the complex geometry of SI model is more generalized as

$$\begin{aligned}
{}^{FFC}D_t^{i,j}S(t) &= (r-\mu)S(t) - \Omega_1 S^2(t) - (\Omega_2+\beta)S(t)I(t) + \eta I(t),\\
{}^{FFC}D_t^{i,j}I(t) &= (\beta-\Omega_4)S(t)I(t) - \Omega_3 I(t)^2 - (\eta+\mu)I(t),\\
S(0) &= S_0,\ I(0) = I_0.
\end{aligned} \tag{1.2}$$

As for the novelty of the paper, it lies in considering the dynamics of a single species' density in relation to the spread of infection in the environment, alongside competition both with other species and within the species itself. The operator in the sense of Caputo power law having fractal dimension and non-integer order is operated to consider the problem for testing the complex geometry of the healthy and infections dynamics. The total density of the species is divided into two agents of healthy class and the infectious class. For the biological validation, the qualitative analysis is carried out in the sense of fixed point theory. The stability analysis for the solution is also treated by using the Ulam-Hyers concept of stability in the sense of the said operator. The approximate solution scheme has been developed for each quantity along with a graphical representation of different fractional order and fractal dimensions. Using an Artificial Neural Network (ANN) technique, the authors divided the data set into three different categories in this study: training, testing, and validation.

The rest of the paper is organized as follows. Section 2 composes some basic definitions related to the said work. Section 3 presents the derivation of existence and uniqueness of solution for the considered model. Section 4 is for the stability analysis of the solution of the proposed model. Section 5 presents the approximate solution scheme of SI model. Section 6 is about graphical representation of both quantities having different cases with artificial neural network analysis. The concluding remarks are given in Section 7.

2. Basic definitions

Definition 2.1 ([6])**.** The fractal-fractional operator for a derivable mapping $\mathcal{J}$, with non natural order i and fractal dimension j in Caputo sense is given as

$${}^{FFC}D_t^{i,j}(\mathcal{J}(t)) = \frac{1}{(n-i)}\frac{d}{dt^j}\int_0^t (t-s)^{n-i-1}\mathcal{J}(s)ds,$$

for $n-1 < i, j \leqslant n$, where $n \in M$ and $\frac{d\mathcal{J}(s)}{ds^j} = \lim_{t\to 0}\frac{\mathcal{J}(t)-\mathcal{J}(s)}{t^j - s^j}$.

Definition 2.2 ([6])**.** Let $\mathcal{J}(t)$ be defined on $a < t < b$, then the fractal-fractional Caputo order integral of $\mathcal{J}(t)$ with order i is

$${}^{FFC}I^{i,j}\mathcal{J}(t) = \frac{j}{\Gamma(i)}\int_0^t (t-s)^{i-1}s^{j-1}\mathcal{J}(s)ds.$$

Definition 2.3. The system (1.2) is U-H stable if $\exists$ any number $\mathcal{A}_{i,j} \geqslant 0 : \forall\ \varepsilon > 0$ and the total roots $\omega \in A^1(\mathcal{X}, \mathbb{R})$, then the inequality may be defined as $|{}^{FFC}D^{i,j}\omega(t) - \pi(t, \omega(t))| \leqslant \varepsilon$, $t \in \mathcal{X}$, $\mathcal{S} \in A^1(\mathcal{X}, \mathbb{R})$ is the unique root for the said model (1.2), $\ni |\omega(t) - \mathcal{S}(t)| \leqslant \mathcal{A}_{i,j},\ t \in \mathcal{X}$.

Note: we define a closed norm space $\mathscr{D} = (D[0, T], R)$ for the mapping whose norm is given as $\|\omega\| = \max_{t\in[0,T]} |\omega(t)|$ and in particular $\|\omega\| = \|S, I\| = \sup_{t\in[0,T]}\{|S(t)| + |I(t)|\}$.

3. Qualitative analysis of model (1.2)

Here in this part, we study the system (1.2) for existence along with unique root of the system. As the given integration is derivable, hence we write the RHS of system (1.2) as under

$$
\begin{aligned}
{}^{FFC}D^{i}\mathbb{J}(t) &= jt^{j-1}\mathscr{H}_1(S, I, t) = (r-\mu)S(t) - \Omega_1 S(t)^2 - (\Omega_2+\beta)S(t)I(t) + \eta I(t),\\
{}^{FFC}D^{i}I(t) &= jt^{j-1}\mathscr{H}_2(S, It) = (\beta-\Omega_4)S(t)I(t) - \Omega_3 I(t)^2 - (\eta+\mu)I(t).
\end{aligned}
$$

Next, by result of (1.2) and for any $t \in \mathcal{X}$, the said model may be written as

$$
{}^{FFC}D^{i}\omega(t) = jt^{j-1}\phi(t, \omega(t)), \quad 0 < i, j \leqslant 1, \quad \omega(0) = \omega_0. \tag{3.1}
$$

Using the integration of fractal-fractional Caputo sense, the root of (3.1) will be:

$$
\omega(t) = \omega_0(t) + \frac{j}{\Gamma(i)} \int_0^t s^{j-1}(t-z)^{i-1}\phi(s, \omega(s))ds, \tag{3.2}
$$

here

$$
\omega(t) = \begin{cases} S(t), \\ I(t), \end{cases} \qquad \omega_0(t) = \begin{cases} S_0, \\ I_0, \end{cases} \qquad \phi(t, \omega(t)) = \begin{cases} \mathscr{H}_1(S, I, t), \\ \mathscr{H}_2(S, I, t)). \end{cases}
$$

Next, we transform (1.2) to a fixed point operator form and let the operator $T : \mathbb{B} \to \mathbb{B}$ can be defined by

$$
T(\omega)(t) = \omega_0(t) + \frac{j}{\Gamma(j)} \int_0^t s^{j-1}(t-s)^{i-1}\phi(s, \omega(s))ds. \tag{3.3}
$$

To derive the at least results of the said system we apply the theorem as

$$
T(\omega)(t) = \omega_0(t) + \frac{j}{\Gamma(j)} \int_0^t s^{j-1}(t-s)^{i-1}\phi(s, \omega(s))ds. \tag{3.4}
$$

To derive the existence results of the said system we apply the following theorem.

Theorem 3.1. *Let a completely continuous operator* $T : \mathbb{B} \to \mathbb{B}$, $J(T) = \{\omega \in \mathbb{B} : \omega = \nu T(\omega), \nu \in [0, 1]\}$, *is bounded, then* T *has at least one fixed point in* $\mathbb{B}$.

Theorem 3.2. *Consider the operator* $\phi : \mathbb{D} \times \mathbb{B} \to \mathbb{R}$ *is a continuous mapping. Then* T *is "compact".*

Proof. In the first step, we prove that the operator $T : \mathbb{B} \to \mathbb{B}$, given in (3.4), is continuous. Let $\mathbb{A}$ be a bounded set in $\mathbb{B}$, then $\exists \mathcal{A}_\phi > 0$ such that $|\phi(t, \omega(t))| \leqslant \mathcal{A}_\phi$ for all $\omega \in \mathcal{D}$. For any $\omega \in \mathcal{D}$, we have

$$
\begin{aligned}
\|T(\omega)\| &\leqslant \frac{j\mathcal{A}_\phi}{\Gamma(i)} \sup_{t\in[0,T]} \left| \int_0^t (\tau-s)^{i-1}s^{j-1}ds \right| \\
&\leqslant \frac{j\mathcal{A}_\phi}{\Gamma(i)} \sup_{t\in[0,T]} \int_0^t (t-s)^{j-1}s^{i-1}t^{i+j-1}ds \leqslant \frac{j\mathcal{A}_\phi T^{i+j-1}}{\Gamma(i)}\mathbb{D}(i, j),
\end{aligned} \tag{3.5}
$$

so (3.5) shows that T is uniformly bounded, where Beta function can be written as $\mathbb{D}(i, j)$. Next, for equi-continuity of mapping T, for any $t_1, t_2 \in \mathbb{D}$ and $\omega \in \mathbb{A}$, we obtain

$$
\begin{aligned}
\|T(\omega(t_1)+) - T(\omega(t_2))\| &\leqslant \frac{j\mathcal{A}_\phi}{\Gamma(i)} \sup_{t\in[0,T]} \left| \int_0^{t_1} (t_1-s)^{i-1}s^{j-1}ds - \int_0^{t_2} (t_2-s)^{i-1}s^{j-1}ds \right| \\
&\leqslant \frac{j\mathcal{A}_\phi \mathbb{D}(i, j)}{\Gamma(i)}(t_1^{i+j-1} - t_2^{i+j-1}) \to 0 \quad \text{as} \quad t_1 \to t_2.
\end{aligned}
$$

Hence, T is equi-continuous and mapping T is continuous and bounded, therefore, by “Arzelá-Ascoli" result the mapping T is relatively compact which implies completely continuous. □

Next, we apply the following assumption:

(**A**) $\exists$ a fixed $\mathcal{L}_\phi > 0 \ni$ such that for all ω, $\bar{\Psi} \in \mathbb{F}$, we have $|\phi(t,\omega) - \phi(t,\bar{\Psi})| \leqslant \mathcal{L}_\phi |\omega - \bar{\Psi}|$.

For existence uniqueness, we apply fixed point approach.

Theorem 3.3. *Using the assumption* (**A**) *and if* $\Theta < 1$, *then the system* (1.2) *has a unique solution where* Θ *is defined as*

$$\Theta = \frac{\Theta \mathcal{L}_\phi T^{i+j-1}}{\Gamma(i)} \mathbb{D}(i,j). \tag{3.6}$$

Proof. Let, $\sup_{t\in[0,T]} |\phi(t,0)| = \mathbb{K}_\phi < \infty$,

$$r \geqslant \frac{jT^{i+j-1}\mathbb{D}(i,j)\mathbb{K}_\phi}{\Gamma(i) - jT^{i+j-1}\mathbb{D}(i,j)\mathcal{L}_\phi}.$$

We have to show that $T(\mathbb{A}_r) \subset \mathbb{B}_r$, where $\mathbb{A}_r = \{\omega \in \mathbb{F} : \|\omega\| \leqslant r\}$ and $\omega \in \mathbb{A}_r$, as under

$$\begin{aligned}\|T(\omega)\| &\leqslant \frac{j}{\Gamma(i)} \sup_{t\in[0,T]} \int_0^t s^{j-1}(t-s)^{i-1}\big(|\phi(t,\omega(t)) - \phi(t,0)| + |\phi(t,0)|\big)ds \\ &\leqslant \frac{jT^{i+j-1}\mathbb{D}(i,j)(\mathcal{L}_\phi\|\omega\| + \mathbb{K}_\phi)}{\Gamma(i)} \leqslant \frac{jT^{i+j-1}\mathbb{D}(i,j)(\mathcal{L}_\phi r + \mathbb{K}_\phi)}{\Gamma(i)} \leqslant r.\end{aligned}$$

Consider the mapping $T : \mathbb{B} \to \mathbb{B}$ is defined in (3.4). Using the assumption (**A**) and for all $t \in D$, ω, $\overline{\Psi} \in D$, we obtain

$$\|T(\omega) - T(\overline{\omega})\| \leqslant \frac{j}{\Gamma(i)} \sup_{t\in[0,T]} \left| \int_0^t s^{j-1}(t-s)^{i-1}\phi(s,\omega(s))ds - \int_0^t s^{j-1}(t-s)^{i-1}\phi(s,\overline{\Psi}(s))ds \right| \leqslant \Theta\|\omega - \bar{\Psi}\|.$$

By this, T is “contraction". Therefore, the result (3.2) has unique solution and so the considered system (1.2) has unique root. □

4. Stability analysis

Here in this section, we have to test the Ulam-Hyers stability for the proposed model (1.2) and its solution, for this take $\Psi \in C(D)$ related to solution with $\Psi(0) = 0$. Then

- $|\Psi(t)| \leqslant \xi$ for $\xi > 0$;
- ${}^{FFC}D^{i,j}\omega(t) = \Psi(t,\omega(t)) + \Psi(t)$.

Lemma 4.1. *The root of perturbable equation* ${}^{FFC}D^{i,j}\omega(t) = \Psi(t,\omega(t)) + \Psi(t)$, $\omega(0) = \omega_0$, *satisfies the relation*

$$\left|\omega(t) - \left(\omega_0(t) + \frac{j}{\Gamma(i)}\int_0^t s^{j-1}(t-s)^{i-1}\Psi(s,\omega(s))ds\right)\right| \leqslant \left(\frac{jT^{i+j-1}\mathbb{D}(i,j)}{\Gamma(i)}\right)\xi = \mathbb{D}_{i,j}\xi. \tag{4.1}$$

Theorem 4.2. *With the assumption* (**A**) *and* (4.1), *the solution of the integral equation* (3.2) *is Ulam-Hyers stable and this implies that the solution of the proposed system is Ulam-Hyers stable if* $\Theta < 1$, *where* Θ *is defined in* (3.6).

Proof. Consider $\mathbb{S} \in \mathbb{B}$ be a unique root and $\omega \in \mathbb{B}$ be any root of (3.2), then using fractal-fractional antiderivative as given in an equation (2.2), then we can write

$$\begin{aligned}
|\omega(t) - \mathbb{S}(t)| &= \left|\omega(t) - \left(\mathbb{S}_0(t) + \frac{j}{\Gamma(i)}\int_0^t (t-s)^{i-1}s^{j-1}\Psi(s,\mathbb{S}(s))ds\right)\right| \\
&\leqslant \left|\omega(t) - \left(\omega_0(t) + \frac{j}{\Gamma(i)}\int_0^t (t-s)^{i-1}s^{j-1}\Psi(s,\omega(s))ds\right)\right| + \left|\left(\omega_0(t)\right.\right. \\
&\quad \left.\left.+ \frac{j}{\Gamma(i)}\int_0^t (t-s)^{i-1}s^{j-1}\Psi(s,\omega(s))ds\right) - \left(\mathbb{S}_0(t) + \frac{j}{\Gamma(i)}\int_0^t (t-s)^{i-1}s^{j-1}\Psi(s,\mathbb{S}(s))ds\right)\right| \\
&\leqslant \mathbb{D}_{i,j}\xi + \frac{j^{i+j-1}\mathcal{L}_\omega}{\Gamma(i)}\mathbb{D}(i,j)\|\omega - \mathbb{S}\| \leqslant \mathbb{D}_{i,j} + j\|\omega - \mathbb{S}\|.
\end{aligned}$$

Now this implies

$$\|\omega - \mathbb{S}\| \leqslant \mathbb{D}_{i,j} + j\|\omega - \mathbb{S}\|. \tag{4.2}$$

From (4.2), we have

$$\|\omega - \mathbb{S}\| \leqslant \left(\frac{\mathbb{D}_{i,j}}{1-j}\right)\xi. \tag{4.3}$$

Thus from the above equation (4.3), we concluded that the solution of (3.2) is Ulam-Hyers stable and therefore, the considered system (1.2) solution has Ulam-Hyers. □

5. Numerical scheme

The evaluation of exact solution is very difficult task for most of the real world problems having complexity and non-linearity. Further, the fractional operator makes them more complex because we find out the complex geometrical dynamics in such fields. Therefore, numerical solution using different numerical methods have much more importance in such dynamics to the find the approximate solution along with their prediction in near future. So, we are developing the approximate solution algorithm for the proposed system and for their validation we perform numerical simulation. Here, for numerical method the construction of equation (3.2) of the considered model goes to the following form

$$S(t) = S(0) + \frac{j}{\Gamma(i)}\int_0^t s^{j-1}(t-s)^{i-1}\mathscr{H}_1(S,I,s)ds, \quad I(t) = I(0) + \frac{j}{\Gamma(i)}\int_0^t s^{j-1}(t-s)^{i-1}\mathscr{H}_2(S,I,s)ds. \tag{5.1}$$

Further, we are presenting the approximate solution method to the (5.1) and applying the novel approach t_{r+1}. The first equation of proposed model becomes

$$S_{r+1} = S_0 + \frac{j}{\Gamma(i)}\int_0^{t_{r+1}} s^{j-1}(t_{r+1}-s)^{i-1}\mathscr{H}_1(S,I,s)ds.$$

The above equation implies

$$S_{r+1} = S_0 + \frac{j}{\Gamma(i)}\sum_{z=0}^{r}\int_{t_z}^{t_{z+1}} s^{j-1}(t_{r+1}-s)^{i-1}\mathscr{H}_1(S,I,s)ds. \tag{5.2}$$

For the finite interval $[t_z, t_{z+1}]$ in term of Lagrange's interpolation polynomials the mapping $\mathscr{H}_1(S,I,s)$ along with intervals $\hbar = [t_z - t_{z-1}]$, we obtain

$$S_r^\star \approx \frac{1}{\hbar}\left[(t-t_{z-1})t_z^{j-1}\mathscr{H}_1(S_z,I_z,t_z) - (t-t_z)t_{z-1}^{j-1}\mathscr{H}_1(S_{z-1},I_{z-1},t_{z-1})\right], \tag{5.3}$$

plugging (5.3) into (5.2), then we can write (5.2) as

$$S_{r+1} = S_0 + \frac{j}{\Gamma(i)} \sum_{z=0}^{r} \int_{t_z}^{t_{z+1}} s^{i-1}(t_{k+1} - s)^{i-1} S_r^\star ds. \tag{5.4}$$

By simplification on the right side integral of (5.4), we obtain first class in (1.2) by applying the fractal-fractional derivative in the Caputo form as:

$$\begin{aligned} S_{r+1} = S_0 + \frac{j\hbar^i}{\Gamma(i+2)} \sum_{z=0}^{r} \Big[& t_z^{j-1} \mathscr{H}_1(S_z, I_z, t_z) \Big((r+1z)^j (r-z+2+j) - (r-j)^j (r-z+2+2j) \Big) \\ & - t_{z-1}^{j-1} \mathscr{H}_1(S_{z-1}, I_{z-1} t_{z-1}) \Big((r+1-z)^j + 1 - (r-z)^j (r-z+1+j) \Big) \Big]. \end{aligned}$$

By the same fashion, the remaining quantities can be written as

$$\begin{aligned} I_{r+1} = I_0 + \frac{j\hbar^i}{\Gamma(i+2)} \sum_{z=0}^{r} \Big[& t_z^{j-1} \mathscr{H}_2(S_z, I_z, t_z) \Big((r+1z)^j (r-z+2+j) - (r-j)^j (r-z+2+2j) \Big) \\ & - t_{z-1}^{j-1} \mathscr{H}_2(S_{z-1}, I_{z-1} t_{z-1}) \Big((r+1-z)^j + 1 - (r-z)^j (r-z+1+j) \Big) \Big]. \end{aligned}$$

6. Simulation discussion

Next, we have to graph the two compartments by the developed approximate solution method to check the dynamics of SI model having response of all the data given in Table 1. We chose five cases for simulations and comparison among them for different fractional orders. In the first case we take different fractional orders i and fractal dimension j. Furthermore, the initial numerical values $S(0) = 1.5, I(0) = 0.8$. The used parameter values are given in Table 1 ([14]).

Table 1: Parameters numerical values for model (1.1).

Parameter	D-I	D-II	D-III	D-IV	D-V
r	0.6	0.6	0.6	0.6	0.6
μ	0.1	0.1	0.1	0.1	0.1
ω_1	0.1	0.1	0.4	0.7	0.1
ω_2	0.1	0.1	0.4	0.8	0.1
ω_3	0.1	0.1	0.4	0.8	0.7
ω_4	0.1	0.1	0.4	0.1	0.1
β	0.4	0.1	0.2	0.7	0.4
η	0.1	0.1	0.2	0.4	0.6

The model data set is separated into three distinct categories, with 70% designated for training, 15% for testing, and 15% for validation, based on varying fractional orders. The following figures provide a graphical representation of both classes on various fractional orders and fractional dimensions using Lagrange's interpolation polynomials in the context of FF Caputo and ANN. In Figures 1 (a)-(b), representing the values of data-I, in which we draw the dynamics of susceptible and infected classes on different fractal and fractional order, where time and step size are considered as $t \in [0, 60]$ and $h = 0.01$. The susceptible class population declines after a short growth but they become stable as the infection class is controlled. After the increase occur in infected class they also decline up-to small quantity and then become stable. The performance of the considered model is shown in Figure 2a, with mean square errors of $1.436e-13$ at epoch 12. The error histogram is shown in Figure 2b, where the best value we find for this case is $-2.4e-08$. The best fit of the training and testing data is shown in Figure 2c, along with errors as indicated in the same figure. The regression of the considered model is shown in Figure 3 with training, testing, and for all data. The value of R is around 1, and from these plots, it is clear that all data is on the regression line, indicating that the obtained solution is accurately trained.

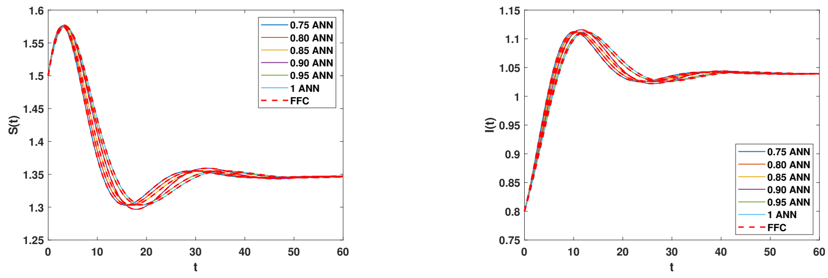

(a) **(b)**

Figure 1: Graphical view of $S(t)$ and $I(t)$ on six different fractional orders, fractal dimension, and parameters values are of data-I with ANN.

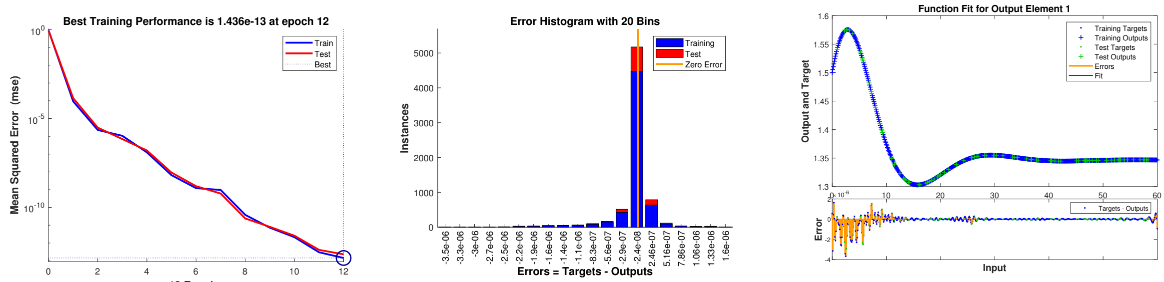

(a) **(b)** **(c)**

Figure 2: Statistically dynamics of the considered model with ANN (a) mean square error; (b) error histogram; and (c) training fit.

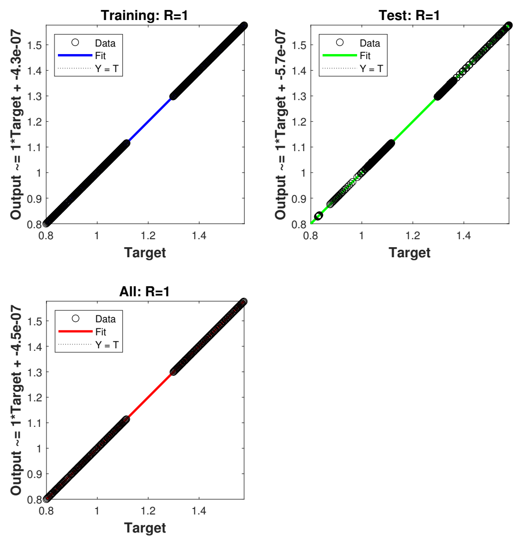

Figure 3: Dynamically representation of the regression with ANN for the considered system.

Next, for Data-II the same dynamics are given in Figures 4 (a)-(b), for time $t \in [0, 60]$ in which the infection is controlled and compared with NN. Figure 5a illustrates the performance of the considered model at epoch 112, with mean square errors of $6.0613e-13$. The error histogram can be shown in Figure 5b, where $206.4e-08$ is the best value we obtain in this particular example. Figure 5c displays the errors as stated in the same figure together with the best fit of the training and testing data. Figure 6 displays the regression of the model under consideration for all data, testing data, and training data. All of the data is clearly on the regression line, demonstrating that the generated solution is accurately trained. The value of R is about 1.

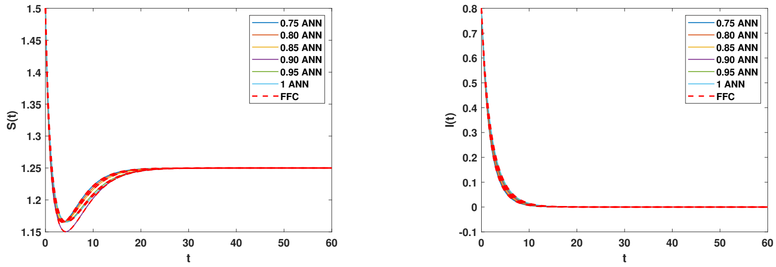

(a) (b)

Figure 4: Graphical view of S(t) and I(t) on six different fractional orders, fractal dimension, and parameters values are of data-II with ANN.

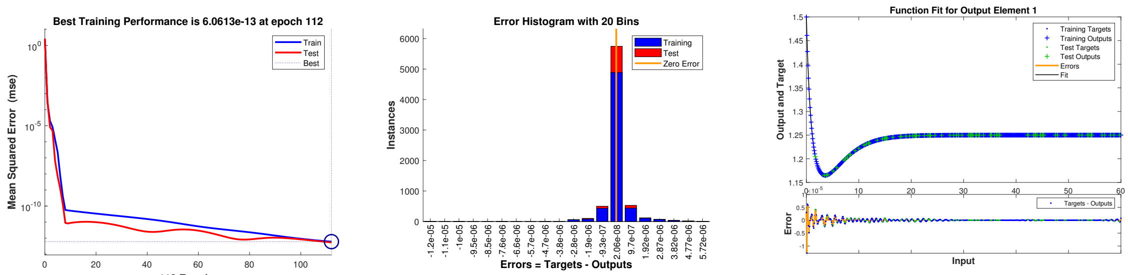

(a) (b) (c)

Figure 5: Statistically dynamics of the considered model with ANN (a) mean square error; (b) error histogram; and (c) training fit.

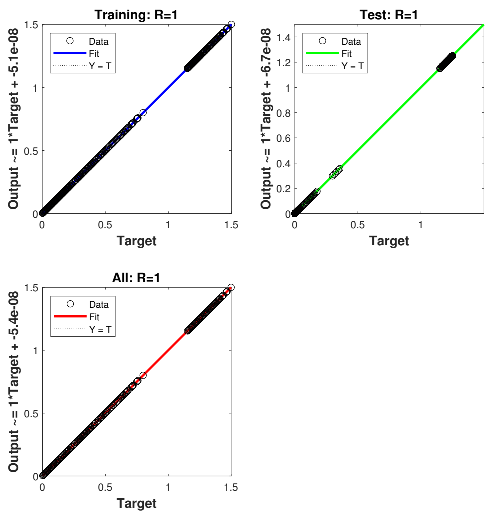

Figure 6: Dynamically representation of the regression with ANN for the considered system.

In figures 7 (a)-(b) the small variation occurs as we use Data-III and NN comparison, respectively.

The performance of the examined model at epoch 505 is shown in Figure 8a, with mean square errors of $3.2263e - 12$. Figure 8b displays the error histogram, with $-1.2e - 06$ being the best number we could find in this case. The errors as indicated in Figure 8c are shown alongside the best fit of the training and testing data. The model under consideration's regression for all, testing, and training data is shown in Figure 9. The produced solution is accurately trained, as evidenced by the fact that all of the data is clearly on the regression line. R has a value of around 1. In Figures 10 (a)-(b) about the same simulation

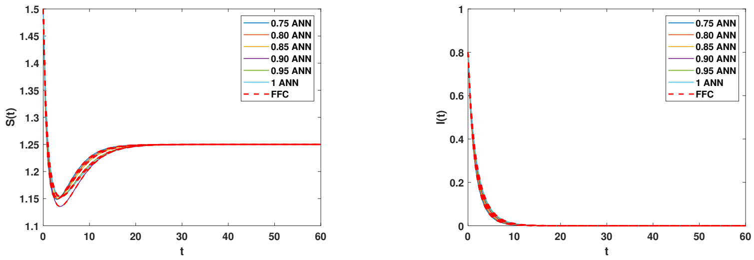

(a) **(b)**

Figure 7: Graphical view of S(t) and I(t) on six different fractional orders, fractal dimension, and parameters values are of data-III with ANN.

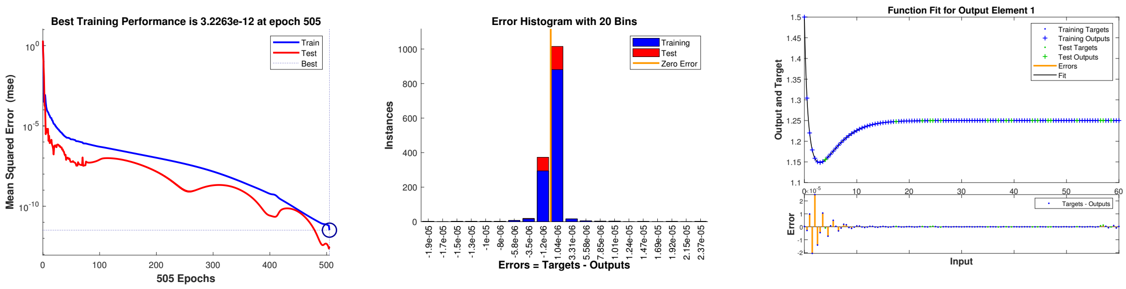

(a) **(b)** **(c)**

Figure 8: Statistically dynamics of the considered model with ANN (a) mean square error; (b) error histogram; and (c) training fit.

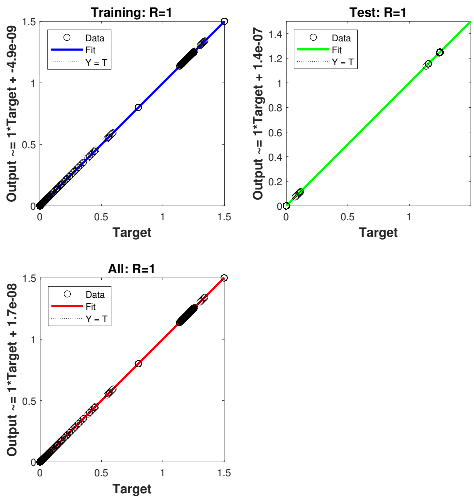

Figure 9: Dynamically representation of the regression with ANN for the considered system.

is shown as in the previous one. These figures represent the dynamics on another set of Data-IV which also affect the said dynamics. Figure 11a displays the model performance at epoch 22, with mean square errors of $9.7032e-10$. The error histogram is shown in Figure 11b, and the best value we could find in this instance was $-8.4e-07$. The best fit of the training and testing data is displayed alongside the errors, as seen in Figure 11c. Figure 12 displays the regression for all, testing, and training data for the model under discussion. All of the data is clearly on the regression line, indicating that the generated solution was accurately trained. R is about equal to 1.

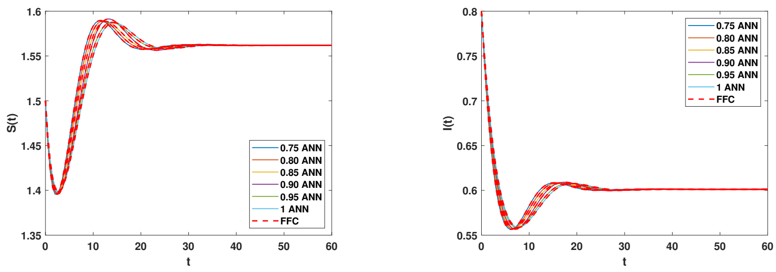

(a) **(b)**

Figure 10: Graphical view of S(t) and I(t) on six different fractional orders, fractal dimension, and parameters values are of data-IV with ANN.

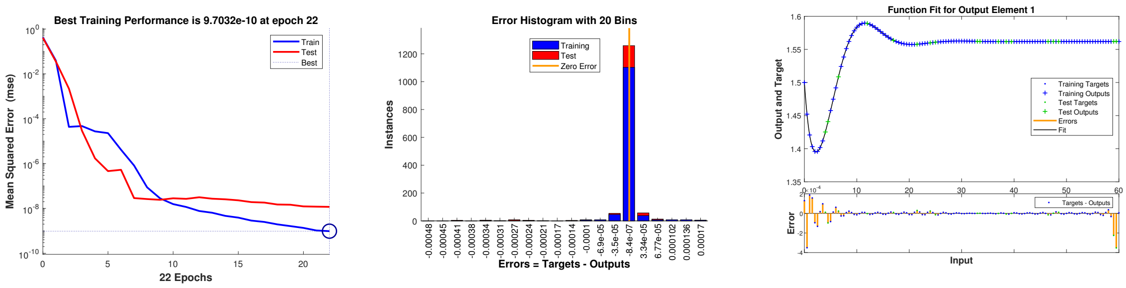

(a) **(b)** **(c)**

Figure 11: Statistically dynamics of the considered model with ANN (a) mean square error; (b) error histogram; and (c) training fit.

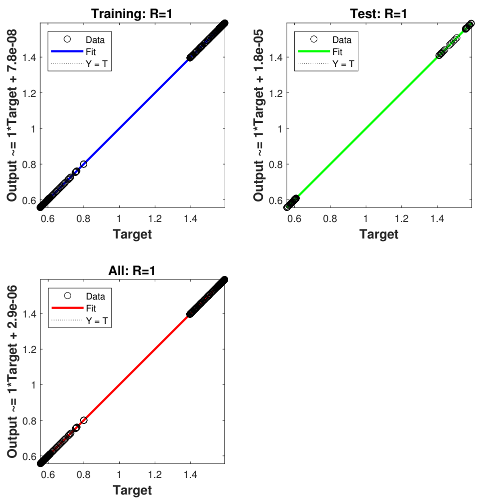

Figure 12: Dynamically representation of the regression with ANN for the considered system.

Figures 13 (a)-(b), the damping dynamics for data-V and comparison the results with NN accordingly are presented. The model performance at epoch 16, with mean square errors of $1.6093e-12$, is shown in Figure 14a. The error histogram can be shown in Figure 14b. In this case, $-9.6e-07$ was the best number we could discover. As seen in Figure 14c, the errors are shown alongside the best fit of the training and testing data. The regression for all, testing, and training data for the model under consideration is shown in Figure 15. Since every piece of data sits squarely on the regression line, the produced solution was precisely trained. R is about equivalent to 1.

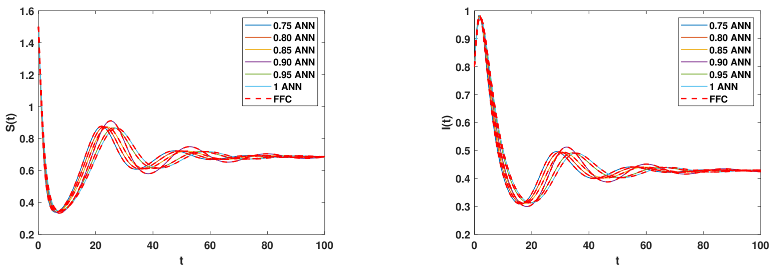

(a) (b)

Figure 13: Graphical view of S(t) and I(t) on six different fractional orders, fractal dimension, and parameters values are of data-V with ANN.

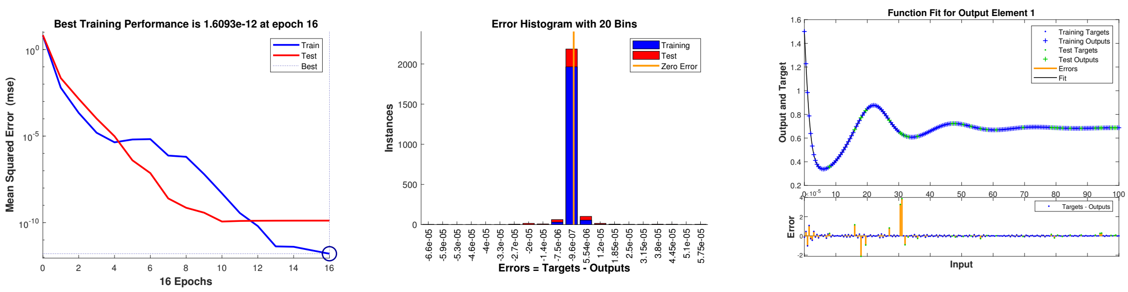

(a) (b) (c)

Figure 14: Statistically dynamics of the considered model with ANN (a) mean square error; (b) error histogram; and (c) training fit.

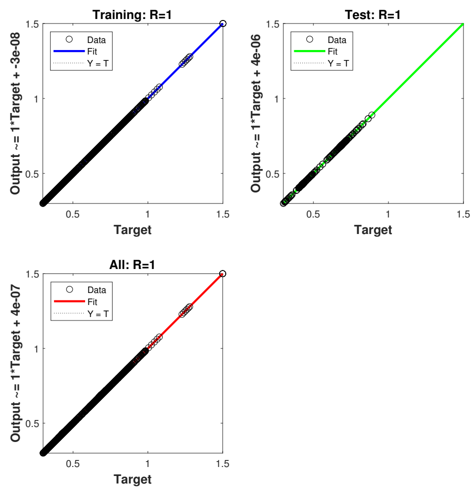

Figure 15: Dynamically representation of the regression with ANN for the considered system.

7. Concluding remarks

The SIS model of healthy population and infected population have been successfully investigated by the effect of competition with each other and other species in the eco-system under the Caputo fractal fractional operator for the complex geometry of the system. The said model validity is shown by the existence and uniqueness of solution along with the Ulam-Hyers stability techniques for the stability of solution. The developed numerical scheme is verified by the graphical solution for both the cases on six different fractional orders and fractal dimensions showing extra degree of choice for each quantity. The rate of infection and rate of death due to competition in the environment are the main factors for instability showing the biological interpretation in the mathematical findings. The used analysis are very helpful and will easily applicable for other such type of epidemiological study and predator-prey systems. Additionally, we used the ANN approach and used graphics to compare the outcomes with those produced using the PCC method. Three subsets of the dataset were created: training, testing, and validation. It is clear from both performance evaluation and graphical analysis that the solution is correctly taught.

Acknowledgment

The authors extend their appreciation to Prince Sattam bin Abdulaziz University for funding this research work through the project number (PSAU/2024/01/99517).

References

[1] M. S. Abdo, T. Abdeljawad, S M. Ali, K. Shah, *On fractional boundary value problems involving fractional derivatives with Mittag-Leffler kernel and nonlinear integral conditions*, Adv. Differ. Equ., **2021** (2021), 1–21. 1
[2] C. Arancibia-Ibarra, P. Aguirre, J. Flores, P. van Heijster, *Bifurcation analysis of a predator-prey model with predator intraspecific interactions and ratio-dependent functional response*, Appl. Math. Comput., **402** (2021), 20 pages. 1
[3] M. Arfan, H. Alrabaiah, M. Ur Rahman, Y.-L. Sun, A. S. Hashim, B. A. Pansera, A. Ahmadian, S. Salahshour, *Investigation of fractal-fractional order model of COVID-19 in Pakistan under Atangana-Baleanu Caputo (ABC) derivative*, Results Phys., **24** (2021), 1–11. 1
[4] A. Aswad, A. Katzourakis, *The first endogenous herpesvirus, identified in the tarsier genome, and novel sequences from primate rhadinoviruses and lymphocryptoviruses*, PLoS Genet., **10** (2014), 1–17. 1
[5] A. Atangana, *Fractal-fractional differentiation and integration: connecting fractal calculus and fractional calculus to predict complex system*, Chaos Solitons Fractals, **102** (2017) 396–406.
[6] A. Atangana, *Modelling the spread of COVID-19 with new fractal-fractional operators: can the lockdown save mankind before vaccination?*, Chaos Solitons Fractals, **136** (2020), 38 pages. 1, 2.1, 2.2
[7] A. Atangana, E. F. D. Goufo, *Some misinterpretations and lack of understanding in differential operators with no singular kernels*, Open Phys., **18** (2020) 594–612. 1
[8] D. Baleanu, A. Jajarmi, H. Mohammadi, S. Rezapour, *A new study on the mathematical modelling of human liver with Caputo-Fabrizio fractional derivative*, Chaos Solitons Fractals, **134** (2020), 7 pages. 1
[9] D. Bhattacharjee, A. J. Kashyap, H. K. Sarmah, R. Paul, *Dynamics in a ratio-dependent eco-epidemiological predator-prey model having cross species disease transmission*, **2021** (2021), 45 pages 1
[10] E. N. Bodine, A. E. Yust, *Predator-prey dynamics with intraspecific competition and an Allee effect in the predator population*, Lett. Biomath., **4** (2017), 23–38. 1
[11] F. Brauer, *Mathematical epidemiology: Past, present, and future*, Infect. Dis. Model. **2** (2017), 113–127. 1
[12] H. Cao, H. Wu, X. Wang, *Bifurcation analysis of a discrete SIR epidemic model with constant recovery*, Adv. Differ. Equ., **2020** (2020), 20 pages. 1
[13] I. Darti, A. Suryanto, H. S. Panigoro, H. Susanto, *Forecasting COVID-19 epidemic in Spain and Italy using a generalized Richards model with quantified uncertainty*, Commun. Biomath. Sci., **3** (2020), 90–100. 1
[14] I. Djakaria, H. S. Panigoro, E. Bonyah, E. Rahmi, W. Musa, *Dynamics of SIS-epidemic model with competition involving fractional-order derivative with power-law kernel*, Commun. Math. Biol. Neurosci., **2022** (2022), 29 pages. 1, 6
[15] F. F. Eshmatov, U. U. Jamilov, Kh. O. Khudoyberdiev, *Discrete time dynamics of a SIRD reinfection model*, Int. J. Biomath., **16** (2023), 22 pages. 1
[16] H. W. Hethcote, *The mathematics of infectious diseases*, SIAM Rev., **42** (2000), 599–653. 1
[17] R. Hilfer, *Applications of fractional calculus in physics*, World Scientific, Singapore, (2000). 1
[18] W. O. Kermack, A. G. McKendrick, *A contribution to the mathematical theory of epidemics*, Proc. R. Soc. Lond. A, **115** (1927), 700–721. 1

[19] S. Kumar, H. Kharbanda, *Sensitivity and chaotic dynamics of an eco-epidemiological system with vaccination and migration in prey*, Braz. J. Phys., **51** (2021), 986–1006. 1
[20] D. Kumar, J. Singh, D. Baleanu, *A new analysis of the Fornberg-Whitham equation pertaining to a fractional derivative with Mittag-Leffler-type kernel*, Eur. Phys. J. Plus, **133** (2018), 1–10. 1
[21] V. Lakshmikantham, S. Leela, J. Vasundhara Devi, *Theory of Fractional Dynamic Systems*, Cambridge Academic Publishers, Cambridge, UK, (2009). 1
[22] B. Li, C. Qin, X. Wang, *Analysis of an SIRS epidemic model with nonlinear incidence and vaccination*, Commun. Math. Biol. Neurosci., **2020** (2020), 14 pages. 1
[23] M. Liu, X. Fu, D. Zhao, *Dynamical analysis of an SIS epidemic model with migration and residence time*, Int. J. Biomath., **14** (2021), 18 pages. 1
[24] J. Liu, B. Liu, P. Lv, T. Zhang, *An eco-epidemiological model with fear effect and hunting cooperation*, Chaos Solitons Fractals, **142** (2021), 13 pages. 1
[25] X. Liu, K. Zhao, J. Wang, H. Chen, *Stability analysis of a SEIQRS epidemic model on the finite scale-free network*, Fractals, **30** (2022), 13 pages. 1
[26] M. Lu, C. Xiang, J. Huang, *Bogdanov-Takens bifurcation in a SIRS epidemic model with a generalized nonmonotone incidence rate*, Discrete Contin. Dyn. Syst. Ser. S, **13** (2020), 3125–3138. 1
[27] A. Miao, X. Wang, T. Zhang, W. Wang, B. G. Sampath Aruna Pradeep, *Dynamical analysis of a stochastic SIS epidemic model with nonlinear incidence rate and double epidemic hypothesis*, Adv. Differ. Equ., **2017** (2017), 27 pages. 1
[28] D. Mukherjee, *Role of fear in predator-prey system with intraspecific competition*, Math. Comput. Simul., **177** (2020), 263–275. 1
[29] B. H. Mulia, S. Mariya, J. Bodgener, D. Iskandriati, S. R. Liwa, T. Sumampau, J. Manansang, H. S. Darusman, S. A. Osofsky, N. Techakriengkrai, M. Gilbert, *Exposure of Wild Sumatran Tiger (Panthera tigris sumatrae) to Canine Distemper Virus*, J. Wildl. Dis., **57** (2021), 464–466. 1
[30] M. M. Ojo, O. J. Peter, E. F. D. Goufo, H. S. Panigoro, F. A. Oguntolu, *Mathematical model for control of tuberculosis epidemiology*, J. Appl. Math. Comput., **69** (2023), 69–87. 1
[31] J. Philippa, R. Dench, *Infectious diseases of orangutans in their home ranges and in zoos*, In: Fowler's Zoo and Wild Animal Medicine Current Therapy, Elsevier, **9** (2019), 565–573. 1
[32] I. Podlubny, *Fractional differential equations*, Academic Press, San Diego, CA, (1999). 1
[33] S. Qureshi, N. A. Rangaig, D. Baleanu, *New numerical aspects of Caputo-Fabrizio fractional derivative operator*, Mathematics, **7** (2019), 1–14. 1
[34] R. Sanft, A. Walter, *Exploring mathematical modeling in biology through case studies and experimental activities*, Academic Press, London, (2020). 1
[35] M. Skoric, V. Mrlik, J. Svobodova, V. Beran, M. Slany, P. Fictum, J. Pokorny, I. Pavlik, *Infection in a female Komodo dragon (Varanus komodoensis) caused by Mycobacterium intracellulare: A case report*, Vet. Med., **57** (2012), 163–168. 1
[36] M. ur Rahman, S. Ahmad, R. T. Matoog, N. A. Alshehri, T. Khan, *Study on the mathematical modelling of COVID-19 with Caputo-Fabrizio operator*, Chaos Solitons Fractals, **150** (2021), 9 pages. 1
[37] M. ur Rahman, M. Arfan, Z. Shah, E. Alzahrani, *Evolution of fractional mathematical model for drinking under Atangana-Baleanu Caputo derivatives*, Phys. Scr., **96** (2021). 1
[38] D. Zhao, S. Yuan, H. Liu, *Random periodic solution for a stochastic SIS epidemic model with constant population size*, Adv. Differ. Equ., **2018** (2018), 9 pages. 1